THE JOURNAL OF SEXUAL MEDICINE
An Official Journal of The International Society for Sexual Medicine

Phosphodiesterase type 5 inhibitors and selective oestrogen receptor modulators can prevent but not reverse myofibroblast transformation in Peyronie's disease

Journal:	*Journal of Sexual Medicine*
Manuscript ID	JSM-20-296.R1
Article type:	Original Research
Keywords:	Myofibroblast transformation, Peyronie's disease, PDE5i, SERM, transforming growth factor, Fibrosis
Subject Area:	Basic science molecular
Abstract:	Background: Myofibroblast transformation is a key step in the pathogenesis of Peyronie's disease (PD). Phosphodiesterase type 5 inhibitors (PDE5i) and selective oestrogen receptor modulators (SERMs) can prevent the formation of fibrosis in in vitro and in vivo models of PD. However, it is unknown whether these drugs can also reverse established fibrosis. Aim: To investigate whether PDE5i and SERMs can reverse transforming growth factor beta 1 (TGF-β1)-induced myofibroblast transformation and determine the point of no return. Methods: In-Cell ELISA (ICE) was used to quantify TGF-β1-induced myofibroblast transformation of human primary fibroblasts isolated from tunica albuginea (TA) of patients undergoing surgery for treatment of PD. ECM production and collagen contraction assays were used as secondary assays. Reverse transcription quantitative polymerase chain reaction (RT-qPCR) and ICE were utilised to measure drug target expression. PDE5i (vardenafil) and SERM (tamoxifen) were applied at various time points following TGF-β1. Outcomes: Reversibility of myofibroblast transformation and drug target expression were investigated in a time dependent manner in TA-derived fibroblasts Results: Vardenafil or tamoxifen could not reverse the myofibroblast traits of alpha-smooth muscle actin (ASMA) expression and extracellular matrix production, whilst only tamoxifen affected collagen contraction after 72h of TGF-β1 treatment. PDE5A and Oestrogen receptor (ER)-β were downregulated after 72h, ER-α protein could not be quantified. Tamoxifen could prevent myofibroblast transformation until 36h after TGF-β1 treatment, vardenafil only 24h after TGF-β1 treatment. This was mirrored by downregulation of drug targets on mRNA and protein level. Further anti-fibrotic signalling pathways, peroxisome proliferator-activated receptor gamma (PPARy) and betaglycan (TGFBRIII), were significantly downregulated after 36h of TGF-β1 exposure, as opposed to upregulation of pro-fibrotic thrombospondin-1 (THSB-1) at the same time point. Clinical Translation: This study suggests that using PDE5i and SERMs might only help for early phase Peyronie's disease and further highlights the need to test drugs at the appropriate stage of the disease based on

	their mechanism of action. Strengths & Limitations: The study utilises primary human TA-derived fibroblasts which enhances translatability of the results. Limitations include that only one example of PDE5i- and SERM- type drug was tested. Time course experiments were only performed for marker expression experiments and not for functional assays. Conclusion: This is the first study to demonstrate that timing for administration of drugs affecting myofibroblast transformation appears to be vital in in vitro models of Peyronie's disease, where 36h of TGF-β1 treatment can be suggested as a "point of no return" for myofibroblast transformation.

1. Conflicts of Interest: No
2. Statement: CUST_CONFLICT_-_YES :No data available.

Phosphodiesterase type 5 inhibitors and selective oestrogen receptor modulators can prevent but not reverse myofibroblast transformation in Peyronie's disease

Abstract:

Background: Myofibroblast transformation is a key step in the pathogenesis of Peyronie's disease (PD). Phosphodiesterase type 5 inhibitors (PDE5i) and selective oestrogen receptor modulators (SERMs) can prevent the formation of fibrosis in *in vitro* and *in vivo* models of PD. However, it is unknown whether these drugs can also reverse established fibrosis.

Aim: To investigate whether PDE5i and SERMs can reverse transforming growth factor beta 1 (TGF-β1)-induced myofibroblast transformation and determine the point of no return.

Methods: In-Cell ELISA (ICE) was used to quantify TGF-β1-induced myofibroblast transformation of human primary fibroblasts isolated from tunica albuginea (TA) of patients undergoing surgery for treatment of PD. ECM production and collagen contraction assays were used as secondary assays. Reverse transcription quantitative polymerase chain reaction (RT-qPCR) and ICE were utilised to measure drug target expression. PDE5i (vardenafil) and SERM (tamoxifen) were applied at various time points following TGF-β1.

Outcomes: Reversibility of myofibroblast transformation and drug target expression were investigated in a time dependent manner in TA-derived fibroblasts

Results: Vardenafil or tamoxifen could not reverse the myofibroblast traits of alpha-smooth muscle actin (ASMA) expression and extracellular matrix production, whilst only tamoxifen affected collagen contraction after 72h of TGF-β1 treatment. PDE5A and Oestrogen receptor (ER)-β were downregulated after 72h, ER-α protein could not be quantified. Tamoxifen could prevent myofibroblast transformation until 36h after TGF-β1 treatment, vardenafil only 24h after TGF-β1 treatment. This was mirrored by downregulation of drug targets on mRNA and protein level. Further anti-fibrotic signalling pathways, peroxisome proliferator-activated receptor gamma (PPARγ) and betaglycan (TGFBRIII), were significantly downregulated after 36h of TGF-β1 exposure, as opposed to upregulation of pro-fibrotic thrombospondin-1 (THSB-1) at the same time point.

Clinical Translation: This study suggests that using PDE5i and SERMs might only help for early phase Peyronie's disease and further highlights the need to test drugs at the appropriate stage of the disease based on their mechanism of action.

Strengths & Limitations: The study utilises primary human TA-derived fibroblasts which enhances translatability of the results. Limitations include that only one example of PDE5i- and SERM- type drug was tested. Time course experiments were only performed for marker expression experiments and not for functional assays.

Conclusion: This is the first study to demonstrate that timing for administration of drugs affecting myofibroblast transformation appears to be vital in *in vitro* models of Peyronie's disease, where 36h of TGF-β1 treatment can be suggested as a "point of no return" for myofibroblast transformation.

KEYWORDS: Myofibroblast transformation, Peyronie's disease, transforming growth factor, anti-fibrotic therapies, PDE5i, SERM

Introduction:

Fibrosis is defined as the excess accumulation of extracellular matrix (ECM) proteins in response to chronic injury or inflammation [1]. Fibrotic disorders encompass a wide range of clinically relevant diseases, affecting any organ or system in the body, such as skin, liver, kidney or lung [2–5]. Peyronie's disease (PD) is characterised by the formation of a fibrotic plaque in the penile tunica albuginea (TA) leading to pain, curvature and erectile dysfunction [6]. Despite affecting 0.3-9% of men worldwide [7–9], current medical treatment is very limited. Specifically, there are no approved drugs for the early, unstable phase of PD. To aid drug development endeavours and pre-clinical research, *in vitro* modelling of PD has often been attempted by using TA-derived fibroblasts from patients suffering from PD.

Myofibroblasts are highly contractile and proliferative, alpha-smooth muscle actin (ASMA) positive, ECM producing cells. They are derived from quiescent tissue resident fibroblasts [10] and play a key role in the formation and pathophysiology of PD and fibrosis in general [11]. Whilst being vital in the physiological wound healing response, they are responsible for the plaque formation and subsequent contraction in PD [12,13]. Furthermore, due to their role as main modulators of tissue remodelling and matrix homeostasis, they have been described as critical effectors in fibrosis where their persistence leads to resistance to apoptosis [14,15]. Whilst multiple origins of the myofibroblast have been proposed, the most common source remain locally resident fibroblasts undergoing transformation to myofibroblasts [16].

TGF-β1 is a crucial regulator of fibroblast phenotype and function and is the main effector cytokine in myofibroblast transformation [17]. The canonical signalling pathway for TGF-β1 activates SMAD (Mothers against decapentaplegic homolog) transcriptional activator-dependent which regulate myofibroblast transformation by directly influencing the expression of ACTA2, the gene for the myofibroblast marker ASMA [18]. Additionally, TGF-β1 can act via non-canonical ways, independent of Smad signalling and through crosstalk with other signalling pathways [19,20].

Along with directly targeting TGF-β1-signalling, the inhibition of myofibroblasts has been suggested as a therapeutic approach and recent research has focused on preventing their formation [21–23]. Previously the anti-fibrotic effect of phosphodiesterase type 5 inhibitors (PDE5i) and selective oestrogen receptor modulators (SERMs) has been demonstrated in models of PD [23]. This study showed that PDE5i and SERMs were able to prevent TGF-β1-induced myofibroblast transformation on a phenotypic (reduced ASMA expression) and functional level (reduced ECM formation and contractile ability) in TA-derived cells. However, this study did not address whether the drugs had the ability to reverse already formed fibrosis, e.g. by inducing dedifferentiation, which has been proposed as a

promising alternative in facing the challenges of drug development to tackle fibrotic diseases [24]. Several agents have been reported to achieve a return to non-myofibroblast state, such as capsaicin [25], CU/Zn SOD [26], or S-nitrosothiols [27] but no study has looked at the direct influence of TGF-β1 exposure time on preventing myofibroblast transformation when testing drugs. It is unclear whether drug treatment targeting myofibroblasts might even be more successful during the process of myofibroblast differentiation, as opposed to before or after. Consequently, the primary aim of this study was to investigate whether the previously discovered anti-myofibroblast effect of PDE5i and SERMs is limited to preventing myofibroblast transformation or whether they can also reverse already formed myofibroblasts. A second aim was to investigate the efficacy of PDE5i and SERMs after various times of TGF-β1 exposure and determine a point of no return after TGF-β1 treatment, where it has become impossible for the drugs to reverse or prevent the myofibroblast state.

Methods:

Sample acquisition

Tunica albuginea (TA) tissue samples that would have otherwise been surgical discarded were acquired from patients undergoing corrective surgery for PD at XXXXXX Hospital (XXX), XXXXX. Non-plaque TA was obtained from PD patients undergoing a Nesbit procedure whereby non-fibrotic TA tissue was excised from the opposite side of the plaque. The patients enlisted for this study were aged between 18 and 75, able to understand the patient information sheet and to give written consent. Ethical approval was obtained by independent research ethics committees (XXXXXXX and XXXXX).

Isolation of fibroblasts from TA tissue

Isolation of fibroblasts was performed as previously described [22,23]. Tissue samples were dissected into small pieces to ensure corpus cavernosum was removed, submerged in culture media (DMEM (GIBCO, Invitrogen, Waltham, Massachusetts, United States), 10% FCS (Fisher Scientific, Loughborough, United Kingdom), 1%Pen/Strep (GIBCO, Invitrogen) in 6-well plates and incubated at 37°C, 5% CO_2 in a humidified atmosphere for 5-7 days until cellular outgrowth was observed. Tissue was removed and cells were washed with PBS and fresh, warm medium was added. Cells were incubated at 37°C until they reached 50-70% confluence, after which cultures were expanded. Cells were characterised as previously described[22,23]. Briefly, cells were subjected to RT-qPCR, Immunocytochemistry, In-Cell ELISA, and Western blot to measure expression of mesenchymal marker vimentin, in absence of smooth muscle marker desmin with expression of myofibroblast marker ASMA in TGF-β1 concentration dependent manner. Passages 2-6 were used throughout these experiments.

In-Cell ELISA (ICE)

The expression of ASMA and other protein markers was quantified in 96-well plates using the In-Cell ELISA (ICE) technique, as previously described [22,23]. Fibroblasts were either untreated or pre-treated with 10ng/mL of TGF-β1 for 72h to generate myofibroblast cultures. Cells were seeded onto 96 well optical flat bottom black microplates (Nunc, Rochester, New York, United States) at 5.0 x 10^3 cells /well and left overnight at 37°C, 5% CO_2. Media was replaced with fresh media with and without TGF-β1 (10 ng/ml) for the indicated time points hours. Additionally, a SERM (tamoxifen, Sigma-Aldrich, Gillingham, United Kingdom) or PDE5i (vardenafil, Sigma-Aldrich, UK) was added at different concentrations (0.1 µM to 1,000 µM for PDE5i, 0.018 µM to 54 µM for SERM). SB-505124, a TGFBRII inhibitor was used as control. The compounds were dissolved in 100% DMSO to stock concentration. After incubation, cells were fixed using 4% paraformaldehyde for 20 minutes at room temperature, washed with 0.1% Triton X-100 in PBS and blocked for 90 min using 10% donkey serum plus 0.1%

Triton X-100 in PBS. Primary antibody solution diluted in PBS (1:3,000 dilution of mouse monoclonal anti-ASMA antibody, 1:100 dilution of rabbit monoclonal anti-PDE5A, 1:500 dilution of rabbit polyclonal oestrogen receptor alpha or 1:500 dilution of rabbit polyclonal oestrogen receptor beta) was added and incubated for 2h at room temperature. Additionally, blocking peptides specific to antibodies were used to ensure specificity of antibodies. Blocking peptides were obtained by Abcam (Cambridge, UK). Cells were subjected to three washing steps using 0.1% Tween 20 in PBS after which the secondary antibody and nuclear stain were added (donkey anti-mouse or donkey anti-rabbit at 1:500 which emits at 800 nm; IRdye 800CW; Li-COR, Cambridge, United Kingdom; nuclear counterstain at 1:1,000 that emits at 700 nm (DRAQ5, Biostatus, Loughborough, United Kingdom)) After 1h incubation, cells were washed three times with 0.1% Tween 20 in PBS and the plate was scanned using an infrared imaging system (Odyssey® CLx imager, Li-Cor, UK) at both 700 nm and 800 nm wavelengths.

Immunocytochemistry

Cells were seeded into wells of a 6 well plate containing sterile glass coverslips at 5.0 x 10^4 cells/well. After overnight incubation, media was replaced with either fresh media or media containing TGF-β1 (10 ng/mL; Sigma Aldrich UK) for 72 hours. Cells were fixed using ice cold methanol at -25°C. Coverslips were incubated with 10% donkey serum (Millipore, Burlington, Massachusetts, United States) in PBS and then with a mouse monoclonal anti-α-SMA antibody (1:1,000; Sigma Aldrich, UK), a monoclonal anti-vimentin antibody (1:1,000; Abcam, UK) or a monoclonal anti-desmin antibody (1:100; Abcam, UK). The secondary antibodies used were a donkey anti-mouse secondary antibody (1:250; Millipore, UK) and donkey anti-rabbit secondary antibody (1:250; Millipore, UK). Images were captured using a Zeiss LSM 510 confocal microscope. Images were quantified where applicable by using ImageJ software to assess the corrected total cell fluorescence (CTCF). The formula for CTCF can be found below.

$$CTCF = integrated\ density - (area\ of\ cell * mean\ fluorescence\ background\ reading)$$

CTCF results were normalized as percentage of untreated control cells.

Collagen gel contraction assay

Cell Contraction Assay (Cell Biolabs Inc., San Diego, California, United States) was used according to the manufacturer's instructions as previously described [23]. Cells were treated with 10ng/mL of TGF-β1 prior to the experiments. Contraction experiments lasted over a period of 8h and images were taken every hour using a digital camera (Canon Digital IXUS 55, 5.0 mega pixels). Image analysis was performed using ImageJ software, measuring the surface area of the contracting collagen lattice.

Contraction was calculated as percentage of the surface of the unreleased lattice. Data is shown as percentage of maximum contraction of vehicle control.

ECM production assay

ECM production assays were performed as previously described [23]. Cells were treated with 10ng/mL of TGF-β1 prior to the experiments. Cells were seeded onto 96 well optical flat bottom black microplates (Nunc, Fisher Scientific, UK) at 5 x 10^3 cells per well. After overnight attachment, they were stimulated compounds for 7 days. DRAQ5 in PBS (1:1,000) was added and cells were incubated for 5 min at 37 °C, 5% CO_2 before scanning the plate to obtain nuclear staining. Cells were then lysed using ammonium hydroxide and ECM was fixed using a solution containing 50% methanol and 7.5% acetic acid for 1h at -20°C. Afterwards ECM was stained either with primary antibodies (collagen I, Abcam; collagen III, Millipore; collagen V, Abcam: fibronectin, Millipore) at 1:1000 for 1h on a shaker, followed by incubation with secondary antibody and scanning the plate using an infrared imaging system (Odyssey CLx imager, LI-COR, UK) at both the 700 nm and 800 nm wavelengths. Results were normalized to the cell number before lysis.

RNA isolation and quality assessment

Cells were seeded into 6 well plates (Nunc, Fisher Scientific, UK) at 5.0 x 10^4 cells/well and incubated with or without 10 ng/ml TGF-β1 for the indicated time points. Total RNA was extracted from cells using the RNeasy Mini Kit (Qiagen, UK), according to the manufacturer's instructions. RNA was resuspended in 40µL of water and stored at -80ºC. RNA was quantified using a Nanodrop (ThermoFisher Scientific, UK) and its integrity was assessed using an Agilent Bioanalyser (Agilent Scientific Instruments, Didcot, United Kingdom). All RNA samples had RIN values of 9 and above.

RT reactions

RNA extracted from two patients was used, with RNA from one patient subjected to replicate RT reactions. 100 ng RNA aliquots were reverse transcribed using two Reverse Transcriptases (Superscript IV (ThermoFisher Scientific, UK) and Ultrascript 2.0 (qPCRBio, London, United Kingdom) in 20 µL reactions using random priming and conditions specified by the manufacturers' RT protocols on a Thermocycler (G-Storm, Pickmere, Knutsford, Cheshire, United Kingdom) with the heated lid set to 112 ºC. For subsequent qPCR reactions, the cDNA preparations were diluted 5-fold with RNase-free water.

qPCR

qPCR assays were carried out in 5 µL reactions containing 1x SensiFast SYBR (Bioline, London, United Kingdom) master mixes, with primers at 300 nmol final concentration and 1 µL of diluted cDNA. Thermal cyclers used were either a CFX Connect (Biorad, Watford, United Kingdom) or an Eco

(PCRMax, Stone, Staffordshire, United Kingdom) programmed as follows: enzyme activation at 95ºC for 30 seconds, followed by 40 cycles of 95ºC for 2 seconds, 60ºC for 2 seconds and 72ºC for 5 seconds, with fluorescence collection at 72ºC. Absence of PCR inhibition was checked by using the SPUD assay to detect changes in Cq with the SPUD artificial template in the reactions containing sample DNA compared to water controls [28].

Analysis of qPCR data

Standard curves were prepared for each assay using 10-fold serial dilutions of PCR amplicons, with amplification efficiencies calculated from the slopes of the dilution curves. Fold-changes were calculated using the ΔΔCq method, modified to include actual amplification efficiencies as recommended by the MIQE guidelines [29]. The statistical analyses for data sets were analysed and graphed using Prism for Mac OS X, version 9.0 (Graphpad Software, San Diego, US).

Statistical Analysis

Data analysis was performed using Microsoft Excel 2013 or GraphPad Prism 7 software. Statistical significance, unless otherwise stated, was calculated using one-way ANOVA and Student's t-test for unpaired means (two-sided). A P value less than 0.05 was considered statistically significant.

The differences between multiple groups in collagen contraction and time course In-Cell ELISA quantification experiments were compared using one-way analysis of variance (ANOVA). Student t test for unpaired means (two sided) was used to compare the difference between two groups in ICC and ICE. Prior to performing this calculation, F test of equality of variances was performed, to ensure that equal variance could be assumed when performing Student t test. A p value of <0.05 was considered statistically significant. Experiments were performed in at least three independent times using samples from at least 3 patients in triplicate wells (N=3). Cells derived from the same three patients were used in all experiments. Results from all experiments were pooled, and the mean values and standard errors of mean were used for statistical analysis.

Results:

PDE5i and SERM cannot reverse TGF-β1 induced myofibroblast marker expression

We have previously shown that PDE5i and SERMs can prevent transformation of TA-derived fibroblasts to myofibroblasts *in vitro* [23]. The effect of PDE5i (vardenafil) and SERM (tamoxifen) on myofibroblast transformation in cells that have been pre-treated with TGF-β1 for 72h was investigated by measuring ASMA protein expression using the ICE method. After 72h of TGF-β1 treatment the cells were treated with varying concentrations of vardenafil or tamoxifen for 72h to assess whether the drugs could reverse expression of the myofibroblast marker ASMA. Figure 1A shows that an exemplar vardenafil only had a minor effect on the expression of ASMA and only at the highest concentration (1,000 μM) where a decrease in cell viability was evident. The effect of tamoxifen on ASMA expression in TGF-β1 pre-treated cells is illustrated in Figure 1B. A decrease in ASMA expression was only observed at the highest concentration of tamoxifen (54 μM) which also showed reduced cell viability. These results suggest that vardenafil or tamoxifen are not able to reverse myofibroblast transformation.

Not all myofibroblast functions can be reversed by PDE5i and SERM

To further investigate whether the PDE5i and SERM influence the myofibroblast functions, the effect of the drugs on the myofibroblast function was assessed. Typical myofibroblast functions include contraction and ECM formation [10] and functional assays to measure these have been described previously [23]. Cells were pre-treated with TGF-β1 for 72h in the experiments shown in Figures 2 and 3. The effect of vardenafil, tamoxifen, and a TGFBRII inhibitor (SB-505124) on production of ECM components collagen I, III, V, and fibronectin is shown in Figure 2. Neither the PDE5i nor the SB-505124 compound had any effect on ECM formation at any concentration (Figure 2A-D), whereas the tamoxifen only had an effect at the highest concentration which has previously been shown to affect cell viability. Collagen contraction assays were utilised to further assess the effect of vardenafil and tamoxifen on myofibroblast function in cells pre-treated with TGF-β1. The TGFBRII inhibitor SB-505124 did not inhibit contraction of myofibroblast-populated collagen lattices (MPCL) at any concentration over the course of the experiment (Figure 3A). The same observation could be made for the vardenafil, that did not decrease the contraction at any concentration over 8h (Figure 3B). Surprisingly, any of the tested tamoxifen concentrations (1, 3, 10 μM) caused a significant ($p<0.05$) decrease in collagen lattice contraction over the course of 8h (Figure 3C).

Completed myofibroblast transformation leads to downregulation of drug targets

To elucidate whether this lack of anti-myofibroblast activity is related to the expression of the drug targets, the expression of PDE5A and oestrogen receptor (ER) α and β was compared between untreated TA-derived fibroblasts and cells exposed to TGF-β1 for 72h. The ICE method was used in conjunction with antibody-specific blocking peptides to quantify protein expression reliably (Figure 4), whereas ICC was used to confirm the findings (Supplementary Figure 1). TGF-β1 exposure caused a significant ($p<0.05$) downregulation of PDE5A in TA-derived fibroblasts compared to untreated cells (Figure 4 A, B; Suppl Fig 1A-C). MCF7 cells were used as a positive control and showed expression of PDE5A, whereas the blocking peptide confirmed specificity of the antibody against PDE5A (Figure 4A, B). Expression of ER-α could not be detected on protein level in TA-derived fibroblasts that were untreated or treated with TGF-β1 for 72h and could only be shown in the positive control MCF7 (Fig 4C; Suppl Fig 1D,E,F). Protein expression of ER-β was significantly downregulated ($p<0.05$) in TA-derived fibroblasts after 72h of TGF-β1 exposure (Figure 4C, F; Suppl Fig 1G,H,I). Specificity of the antibody was ensured via the antibody-specific blocking peptide (Figure 4C). MCF7 cells were used for ICC as positive control for PDE5A and ER-β (Suppl Fig 1 J, K).

Effect of PDE5i and SERMs on myofibroblast transformation after limited TGF-β1 exposure

To assess whether there was a specific timepoint between initial TGF-β1 exposure and fully completed myofibroblast transformation at which PDE5i or SERMs could affect or reverse ASMA expression, time course experiments were performed. It is known that myofibroblast transformation requires a total of 72h for completion [30]. To this end, cells were treated with TGF-β1 for 24h, 36h, or 48h after which it was removed and replaced with one of the drugs for the rest of the 72h incubation. To ensure that limited exposure to TGF-β1 would still lead to complete myofibroblast transformation, TA-derived fibroblasts were used and TGF-β1 was removed after 24h, 36h, 48h, 72h after which ASMA expression was quantified at the end of the 72h period (Supplementary Figure 2). As can be seen, there was no difference in ASMA expression between the different time points, meaning only the initial 24h exposure to TGF-β1 is needed to complete full myofibroblast transformation within a 72h period, so cells don't need to be exposed to TGF-β1 for the entire 72h.

Figure 5 depicts the effect of PDE5i on myofibroblast transformation after different TGF-β1 exposure times. When only treated with TGF-β1 for 24h, a subsequent 48h incubation with vardenafil caused a decrease of ASMA expression, as is evidenced by the inverse sigmoid curve with upper and lower plateau in Figure 5A. PDE5i treatment could not prevent ASMA expression after 36h or 48h of TGF-β1 exposure (Figure 5B,C).

Tamoxifen could be shown to affect myofibroblast transformation after 24h and 36h of TGF-β1 exposure (Figure 6A,B) but not after 48h (Figure 6C). The anti-myofibroblast effect seen when using

5.4, 18 and 54µM of tamoxifen gradually gets weaker with longer TGF-β1 pre-treatment. While the highest concentration (54µM) still had some effect (9% inhibition) after 48h of TGF-β1 treatment, lower concentrations did not inhibit ASMA expression anymore.

To confirm the findings, a complete time course of TGF-β1 with SB-505124 was performed (Suppl Fig 3). SB-505124 has previously been shown to prevent myofibroblast transformation *in vitro* [31]. In our setting, SB-505124 was incapable of affecting ASMA expression in cells that were pre-treated with TGF-β1, regardless of dose or treatment time point, confirming that main response to TGF-β1 signalling takes place within the first 24h.

Time course experiments suggest point of return for myofibroblast transformation is after 36h

To further investigate the effect of TGF-β1 on the expression of drug targets for PDE5i and SERMs, cells were exposed to TGF-β1 for varying time points and mRNA levels of specific genes were quantified and compared to untreated cells. GAPDH was validated as a suitable reference gene, as its expression varied little between control samples and those subjected to TGF-ß1 treatment RNA samples, as shown in Supplementary Figure 4. *ACTA*, the gene for ASMA, was significantly upregulated at 24h, 36h, 48h, and 72h of TGF-β1 treatment (Figure 7A). Significant downregulation of mRNA upon TGF-β1 treatment could be observed for *PDE5A*. The mRNA levels were significantly below the level of technical noise at any point of TGF-β1 treatment (Figure 7B). Despite not being able to measure protein levels of ER-α, the mRNA levels of *ER1* were quantified. As can be seen in Figure 7C, the fold-change for expression ranged within the levels of technical noise for 24h and 36h treatment groups, while 48h showed significant downregulation, which returned to levels of technical noise after 72h (Figure7C). *ER2*, the gene for ER-β, showed significant upregulation of mRNA 24h after TGF-β1 treatment. Following 36h of TGF-β1 treatment, there was no significant differences compared with untreated cells (within the 3-fold level for technical noise), while *ER2* mRNA was significantly downregulated after 48h and 72h of TGF-β1 treatment (Figure 7D).

These findings were complemented with protein quantification using ICE. ASMA, PDE5A and ER-β were quantified after exposing cells to TGF-β1 for 24h, 36, 48h and 72h. Whilst mRNA was upregulated after 24h, protein levels of ASMA were only significantly upregulated ($p<0.05$) after 36h and reached their maximum after 72h (Figure 7E), with no significant differences between 48h and 72h. This suggests that its transcriptional and translational regulation are decoupled. In contrast, the protein levels of PDE5A were immediately significantly reduced ($p<0.05$) after 24h (Figure 7F), in line with the significantly lower levels of mRNA. Longer TGF-β1 treatment lead to further reduction, as levels after 36h were significantly lower compared to 24h and levels after 72h after significantly lower than after 36h and 48h. As the cells utilised in these experiments do not seem to express ER-α (Figure

4, Suppl Fig 1), only levels of ER-β were quantified. Protein levels of ER-β were significantly reduced ($p<0.05$) after 48h and 72h compared to untreated cells, whilst there appeared to be a trend for reduced expression after 36h that did not reach significance (Figure 7G.

Gene expression analysis reveals three additional genes with differential regulation after 36h

Since the protein data for ASMA, PDE5A and ER-β suggested a significant event between 36h and 48h, further pro- and anti-fibrotic signalling pathways were investigated via RT-qPCR. GAPDH was validated as reference gene (Suppl Fig 4). A panel of various marker genes was interrogated (Figure 8, Suppl Fig 5). Three genes were found to follow the pattern of 36 h point of no return: peroxisome proliferator-activated receptor-γ (PPARγ), transforming growth factor beta receptor III (TGFBRIII) and thrombospondin-1 (THSB-1). Figures 8A and B depict the expression of PPARγ and TGFBRIII at various time points after TGF-β1 exposure. Both genes were significantly downregulated after 36h, strengthening the case for a point of no return after 36h of TGF-β1 treatment. The gene for TSP-1 (*THSB-1*) was significantly upregulated after 36h of TGF-β1 treatment (Figure 8C). The other markers tested in this study were either unchanged (*BIRC5*, *GPER2*) over the entire time course, or significantly upregulated (*IGF1, IGFBP3*) or downregulated (*GPER4*) 48h after TGF-β1 insult (Suppl Fig 5).

Discussion

This study reports two major findings (1) the anti-fibrotic effects of PDE5i and SERM are dependent on the time of TGF-β1-exposure, as longer TGF-β1-exposure leads to a decrease in drug efficacy (2) there is a point of no return, which occurs around 36h after TGF-β1 treatment that can be delineated by up- and downregulation of key marker proteins and genes.

Previously both PDE5i and SERMs have been suggested as a treatment for PD [32–37]. We have shown that the combination of both drug classes exerted a synergistic effect in preventing myofibroblast transformation [23]. Interestingly, in our experiments, PDE5i treatment did not reduce ASMA expression in cells pre-treated with TGF-β1 for longer than 24h. This indicates that the drugs can inhibit myofibroblast transformation only at the start of the process and cannot reverse it. It also contradicts a previously published result, where treatment using various concentrations of vardenafil could reverse TGF-β1-induced prostate-derived myofibroblast state [38]. However, that study did not quantify protein levels and cells were treated in the same culture dish for a total of 144h in presence of 1 ng/mL of TGF-β1. In contrast, our protocol included a 72h pre-treatment period with 10 ng/ml TGF-β1 after which cells were seeded onto appropriate plates for treatment with PDE5i or SERM. This difference makes any comparison difficult and could explain differences in outcomes between the studies. Myofibroblast function such as contraction and ECM formation were also unaffected by PDE5i treatment, which is conclusive in the context of PDE5i preventing rather than reversing myofibroblast transformation.

Previously it has been suggested that TA-derived myofibroblast transformation can be prevented by oestrogen signalling through inhibition of Smad and Rho [39]. Previous studies have reported SERMs as a potential anti-fibrotic treatment strategy with evidence gathered from *in vitro* and *in vivo* models suggesting reduction of hepatic [40] and renal [41] fibrosis while improved wound healing could be observed in skin fibrosis [42]. Mechanistically, it has been proposed that in rats SERMs decrease the production of TGF-β1 [43] and inhibit the canonical Smad signalling in mice thereby suppressing myofibroblast transformation [44]. Furthermore, a non-Smad mechanism of action has been proposed via targeting of ERK1/2 and AP-1 transcription factor signalling in primary human skin fibroblasts [45]. Given that these suggested mechanisms all involve pathways that are critical for the induction of myofibroblast transformation but are not indispensable for the maintenance of the myofibroblast state, our observations in the time course experiments (prevention until the 36h mark) can be partially explained.

However, the data of the functional collagen contraction assay needs a more critical review. It was unexpected to observe that tamoxifen was able to influence collagen contraction after TGF-β1 pre-

treatment, in context of the potential mechanism of action (preventing rather than reversing myofibroblast transformation as outlined above). As the other myofibroblast hallmarks of ASMA expression (an important contractile feature) and ECM production have not been reversed by SERM treatment, it is reasonable to conclude that inhibition of contraction alone is not sufficient evidence to suggest that myofibroblast transformation was reversed. We thereby hypothesize that tamoxifen affected only the contractile mechanism of the cells, without actually reversing their myofibroblast state. The literature provides examples for SERM influencing collagen contraction [46,47]. Further, utilising cells derived from palmar fascia of Dupuytren's disease and control patients, it could be shown that tamoxifen was able to inhibit the contraction of the cells in both, fibrotic and non-fibrotic settings [48]. Others used fibroblasts from Dupuytren's disease and carpal tunnel affected fascia and observed a higher basal level of contraction in the diseased cells indicating higher myofibroblast baseline count [49]. This study demonstrated an inhibition of contraction after SERM-treatment which was ascribed to a decrease in TGF-β2 expression. Mechanistically, it has been proposed that treatment with SERM leads to a change of morphology that results in a lack of contraction in cells such as fibroblasts [46] but also cancer cells [50,51]. Mechanical inactivation of fibroblast-like cells by tamoxifen has been described to be mediated via GPER/RhoA with subsequent inactivation of YAP [52]. Given the downregulation of ERs after 72h of TGF-β1 treatment, the possibility of an additional, ER-independent or GPER-driven mechanism of SERM that mainly affects cell morphology, cytoskeletal makeup (rearrangement of intermediate and actin filaments/stress fibres [50]), or mechanosensing of the cells to prevent contraction cannot be excluded.

Collectively, the data point towards PDE5i and SERMs only preventing but not reversing TGF-β1-induced myofibroblast transformation of TA-derived cells *in vitro*. To investigate potential underlying reasons for this effect, the expression of drug targets was quantified in a TGF-β1 and time-dependent manner. We hypothesized that exposure to TGF-β1 would lead to a downregulation of PDE5A and ER α and β, which would prevent the drugs from exerting their anti-fibrotic action due to a lack of drug target availability.

Our results demonstrate that TGF-β1 induces a significant downregulation of PDE5A on mRNA and protein level after 72h of TGF-β1 treatment, which may explain the loss of PDE5i efficacy caused by lack of target expression following TGF-β1 exposure. Interestingly, whilst the mRNA downregulation is already apparent after 24h, the most significant downregulation of PDE5A protein appears after 36h, which coincides with a more significant upregulation of ASMA protein levels. Expression of PDE isoforms PDE4 and PDE5 could previously be determined in fibroblast cultures established from human PD plaques, normal TA, and rat TA [53]. Our data are in conflict with a previous study conducted by Zenzmaier et al that examined the consequences of lentivirus mediated shRNA

knockdown of PDE5 in prostate-derived fibroblasts [38]. That study reported that loss of PDE5 lead to a reversal of the myofibroblast state, while we consider the loss of PDE5 as a marker for myofibroblast transformation. Expression of PDE5 has been reported in both rat and human fibroblasts where it was shown that cells at higher passage, which are more susceptible to spontaneous myofibroblast transformation, show a decreased PDE5 expression [54]. Further one study showed that TGF-β1 treatment lead to a significant downregulation of PDE5A protein expression in HFL-1 cells (roughly 50% reduction) [55], which corroborates our expression results and thereby implies the loss of PDE5i efficacy after TGF-β1 pre-treatment is caused by lack of target expression.

Whilst we can detect expression of ER-α and ER-β mRNA in our primary fibroblasts, only ER-β is expressed at the protein level. This narrows down the potential drug target of SERMs in TA-derived fibroblasts. Protein expression of ER-α could only be demonstrated in MCF7 (a breast cancer cell line isolated from a Caucasian woman) cells which have been reported to express ER-α mRNA and protein [56]. This is in line with previous studies that showed expression of ER-β only in adult human mammary fibroblasts in absence of ER-α[57]. Exposure to TGF-β1 for 72h leads to a significant downregulation of ER-β at the protein level. 24h of TGF-β1 lead to a significant upregulation of ER-β mRNA which did not translate to protein level but could be an attempt of the cell to compensate for or counteract the TGF-β1 signalling. During the time course of TGF-β1 treatment it was indicated that expression of the receptor was significantly downregulated after 48h both on mRNA and protein level, which explains why tamoxifen still had a minor effect on myofibroblast transformation after 36h of TGF-β1 exposure.

Collectively, this supports the hypothesis of TGF-β1-mediated downregulation of the drug targets as the main reason for PDE5i and SERMs being unable to reverse full myofibroblast transformation which is reinforced by the observations of the drugs being able to prevent myofibroblast transformation until the expression of the drug targets is too low (after 36h for PDE5i, 48h for SERMs). Further, the lack of ER-α expression suggests that the anti-fibrotic effect of SERMs may be mediated via ER-β related signalling, a notion supported by evidence in breast cancer in general [58] and reports of the tamoxifen response in ER-α negative cancer being ER-β dependent [59]. In turn, others reports suggest that tamoxifen acts through other intracellular signalling cascades, independent of ER-mediated signalling, such as Smad, ERK [44] [45] or the suppression of TGF-β1 transcription [43]. Studies into the precise mechanism of action are needed to resolve which signalling cascade is responsible for the anti-fibrotic effect of SERM in TA-derived cells.

The results of our study may have clinical implications, as they suggest that treatment with PDE5i or SERMs may be useful in patients with early stage PD and that fully formed plaques are unlikely to be affected by either treatment, as myofibroblast elimination or reversal cannot be achieved. Fibrotic

conditions such as PD are characterised by their relatively slow progression, which poses an inherent issue for early treatment. However, reports suggest that patients do present at earlier stages (within the first three months) and not just with fully formed plaques [60–62].

The significant downregulation of key antifibrotic proteins and upregulation of myofibroblast markers at 36h lead us to use RT-qPCR to investigate the expression of additional genes involved in the fibrotic process. In doing so, our study is the first one to try and establish a point of no return in TGF-β1-induced myofibroblast transformation.

We analysed a panel of genes that are involved in the fibrotic process and that were differentially regulated after TGF-β1 treatment. Within this panel of pro- and anti-fibrotic genes, we observed genes that were unchanged (BIRC5, GPER2), immediately strongly upregulated (IGF1, IGFBP3) and downregulated after 48h. Additionally, we observed that three genes had a differential expression pattern after 36h: PPARγ, TGFBRIII, and THSB-1 which followed the pattern of point of no return we have described above. These three genes have strong evidence of influence in the fibrotic process. We have shown that PPARγ and TGFBRIII mRNA levels were significantly decreased 36 hours after TGF-β1 exposure. Decreased PPARγ levels have been suggested as potential biomarker in skin fibrosis [63], whilst the anti-fibrotic effects of L-carnitine, a drug suggested as treatment for PD [64], are derived from its ability to upregulate PPARγ [65]. Further, PPARγ agonists have been demonstrated to decrease fibrotic responses by opposing TGF-β1 pro-fibrotic signalling (including myofibroblast differentiation) [66] suggesting a vital role of PPARγ in the fibrotic process. TGFBRIII has been shown to be downregulated in fibrotic tissue, whilst its upregulation has been proposed as an anti-fibrotic strategy [67]. This underlines the significance of the downregulation of the receptor after 36h of TGF-β1 exposure, as TGFBRIII can act as an accessory co-receptor to modulate TGF-β1 signalling [68]. Our results showed a significant upregulation of THSB-1 mRNA 36 hours after TGF-β1 exposure. THSB-1 perpetuates fibrotic signalling by activating latent TGF-β1 and has therefore been proposed as a target for anti-fibrotic therapy [69,70] and its upregulation has been reported to predict hypoxia as well as fibrosis [71,72]. In penile tissues, THSB-1 upregulation was attributed to fibrotic changes observed in post-radical prostatectomy erectile dysfunction patients [73]. The upregulation of this gene is therefore an important event in the development of fibrosis and, alongside the downregulation of anti-fibrotic genes at the same time point, further underlines the importance of the 36h mark outlined in this manuscript. Defining what leads to this key event that promotes pro-fibrotic genes and at the same inhibits anti-fibrotic genes after 36h might be a novel target to tackle not only PD but fibrosis in general.

Given that fibrosis has a complex pathology with multiple genes and pathways involved, it will be

necessary to confirm this proposed point of no return by obtaining more complete transcriptomic and proteomic data. This should result in the establishment of gene signatures that will help reveal the full mechanism underlying myofibroblast transformation and lead to the discovery of new druggable targets. We acknowledge this lack of high-volume experimentation as one of the limitations of this study, along with the lack of confirmation on protein level. Further, this study is limited by only testing one exemplar PDE5i and SERM and not investigating the effect the drugs might have on the expression of their respective targets. In addition, it is evident that all *in vitro* models are inherently limited in fully representing the complexity and physiology of fibrosis. Ideally, the data would be supported by both, experimentation in 3D-mulitcellular models using multi-cytokine insults, and *in vivo* experiments.

Conclusions:

This study suggests that PDE5i and SERMs cannot reverse already formed fibrosis and should therefore only be used in early stage patients with PD to obtain an anti-fibrotic effect. We also demonstrate a point of no return for myofibroblast transformation after 36h of TGF-β1 treatment. It is worth investigating whether this point of no return can be a viable novel target for further drug development endeavours, as opposed to only preventing formation of or reversing fully formed fibrosis. Our data further demonstrates the need to design clinical trials that take the mechanism of action of the drug into account, as PDE5i and tamoxifen have only been shown to be successful in the trials that recruited early phase PD patients, which as this data demonstrates will respond better to the drugs.

REFERENCES:

[1] Wynn T. Cellular and molecular mechanisms of fibrosis. J Pathol 2008;214:199–210. doi:10.1002/path.2277.

[2] Li J, Chen J, Kirsner R. Pathophysiology of acute wound healing. Clin Dermatol 2007;25:9–18. doi:10.1016/J.CLINDERMATOL.2006.09.007.

[3] Ebrahimi H, Naderian M, Sohrabpour AA. New Concepts on Pathogenesis and Diagnosis of Liver Fibrosis; A Review Article. Middle East J Dig Dis 2016;8:166–78. doi:10.15171/mejdd.2016.29.

[4] Sato Y, Yanagita M. Resident fibroblasts in the kidney: a major driver of fibrosis and inflammation. Inflamm Regen 2017;37:17. doi:10.1186/s41232-017-0048-3.

[5] Martinez FJ, Collard HR, Pardo A, Raghu G, Richeldi L, Selman M, et al. Idiopathic pulmonary fibrosis. Nat Rev Dis Prim 2017;3:17074. doi:10.1038/nrdp.2017.74.

[6] Gonzalez-Cadavid NF. Mechanisms of Penile Fibrosis. J Sex Med 2009;6:353–62. doi:10.1111/J.1743-6109.2008.01195.X.

[7] Schwarzer U, Sommer F, Klotz T, Braun M, Reifenrath B, Engelmann U. The prevalence of Peyronie's disease: results of a large survey. BJU Int 2001;88:727–30. doi:10.1046/j.1464-4096.2001.02436.x.

[8] Mulhall JP, Creech SD, Boorjian SA, Ghaly S, Kim ED, Moty A, et al. Subjective and objective analysis of the prevalence of Peyronie's disease in a population of men presenting for prostate cancer screening. J Urol 2004;171:2350–3.

[9] Lindsay MB, Schain DM, Grambsch P, Benson RC, Beard CM, Kurland LT. The Incidence of Peyronie's Disease in Rochester, Minnesota, 1950 through 1984. J Urol 1991;146:1007–9. doi:10.1016/S0022-5347(17)37988-0.

[10] McAnulty RJ. Fibroblasts and myofibroblasts: Their source, function and role in disease. Int J Biochem Cell Biol 2007. doi:10.1016/j.biocel.2006.11.005.

[11] Gonzalez-Cadavid NF, Rajfer J. Mechanisms of disease: New insights into the cellular and molecular pathology of Peyronie's disease. Nat Clin Pract Urol 2005;2:291–7. doi:10.1038/ncpuro0201.

[12] Jalkut M, Gonzalez-Cadavid N, Rajfer J. New discoveries in the basic science understanding of Peyronie's disease. Curr Urol Rep 2004. doi:10.1007/s11934-004-0074-y.

[13] Gelfand RA, Vernet D, Kovanecz I, Rajfer J, Gonzalez-Cadavid NF, Gonzalez-Cadavid NF. THE TRANSCRIPTIONAL SIGNATURES OF CELLS FROM THE HUMAN PEYRONIE'S DISEASE PLAQUE AND THE ABILITY OF THESE CELLS TO GENERATE A PLAQUE IN A RAT MODEL SUGGEST POTENTIAL THERAPEUTIC TARGETS. J Sex Med 2015;12:313–327. doi:10.1111/jsm.12760.

[14] Hinz B. The role of myofibroblasts in wound healing. Curr Res Transl Med 2016;64:171–7. doi:10.1016/j.retram.2016.09.003.

[15] Moodley YP, Caterina P, Scaffidi AK, Misso NL, Papadimitriou JM, McAnulty RJ, et al. Comparison of the morphological and biochemical changes in normal human lung fibroblasts and fibroblasts derived from lungs of patients with idiopathic pulmonary fibrosis during FasL-induced apoptosis. J Pathol 2004;202:486–95. doi:10.1002/path.1531.

[16] Hinz B, Phan SH, Thannickal VJ, Galli A, Bochaton-Piallat M-L, Gabbiani G. The Myofibroblast: One Function, Multiple Origins. Am J Pathol 2007;170:1807–16. doi:10.2353/AJPATH.2007.070112.

[17] Leask A, Abraham DJ. TGF-ß signaling and the fibrotic response. FASEB J 2004;18:816–27. doi:10.1096/fj.03-1273rev.

[18] Desmouliere A. Transforming growth factor-beta 1 induces alpha-smooth muscle actin expression in granulation tissue myofibroblasts and in quiescent and growing cultured fibroblasts. J Cell Biol 1993;122:103–11. doi:10.1083/jcb.122.1.103.

[19] Szeto SG, Narimatsu M, Lu M, He X, Sidiqi AM, Tolosa MF, et al. YAP/TAZ Are Mechanoregulators of TGF-β-Smad Signaling and Renal Fibrogenesis. J Am Soc Nephrol 2016;27:3117–28. doi:10.1681/ASN.2015050499.

[20] Grannas K, Arngården L, Lönn P, Mazurkiewicz M, Blokzijl A, Zieba A, et al. Crosstalk between Hippo and TGFβ: Subcellular Localization of YAP/TAZ/Smad Complexes. J Mol Biol 2015;427:3407–15. doi:10.1016/J.JMB.2015.04.015.

[21] Bollong MJ, Yang B, Vergani N, Beyer BA, Chin EN, Zambaldo C, et al. Small molecule-mediated inhibition of myofibroblast transdifferentiation for the treatment of fibrosis. Proc Natl Acad Sci U S A 2017;114:4679–84. doi:10.1073/pnas.1702750114.

[22] Mateus M, Ilg MM, Stebbeds WJ, Christopher N, Muneer A, Ralph DJ, et al. Understanding the Role of Adenosine Receptors in the Myofibroblast Transformation in Peyronie's Disease. J

Sex Med 2018;15:947–57. doi:10.1016/j.jsxm.2018.05.003.

[23] Ilg MM, Mateus M, Stebbeds WJ, Milenkovic U, Christopher N, Muneer A, et al. Antifibrotic Synergy Between Phosphodiesterase Type 5 Inhibitors and Selective Oestrogen Receptor Modulators in Peyronie's Disease Models. Eur Urol 2019;75:329–40. doi:10.1016/j.eururo.2018.10.014.

[24] Yang X, Chen B, Liu T, Chen X. Reversal of myofibroblast differentiation: A review. Eur J Pharmacol 2014;734:83–90. doi:10.1016/J.EJPHAR.2014.04.007.

[25] Yu F-X, Teng Y-Y, Zhu Q-D, Zhang Q-Y, Tang Y-H. Inhibitory effects of capsaicin on hepatic stellate cells and liver fibrosis. Biochem Cell Biol 2014;92:406–12. doi:10.1139/bcb-2014-0036.

[26] Vozenin-Brotons M-C, Sivan V, Gault N, Renard C, Geffrotin C, Delanian S, et al. Antifibrotic action of Cu/Zn SOD is mediated by TGF-β1 repression and phenotypic reversion of myofibroblasts. Free Radic Biol Med 2001;30:30–42. doi:10.1016/S0891-5849(00)00431-7.

[27] Vercelino R, Crespo I, de Souza GFP, Cuevas MJ, de Oliveira MG, Marroni NP, et al. S-nitroso-N-acetylcysteine attenuates liver fibrosis in cirrhotic rats. J Mol Med 2010;88:401–11. doi:10.1007/s00109-009-0577-6.

[28] Nolan T, Hands RE, Ogunkolade W, Bustin SA. SPUD: A quantitative PCR assay for the detection of inhibitors in nucleic acid preparations. Anal Biochem 2006;351:308–10. doi:10.1016/j.ab.2006.01.051.

[29] Bustin SA, Benes V, Garson JA, Hellemans J, Huggett J, Kubista M, et al. The MIQE guidelines: Minimum information for publication of quantitative real-time PCR experiments. Clin Chem 2009;55:611–22. doi:10.1373/clinchem.2008.112797.

[30] Hecker L, Jagirdar R, Jin T, Thannickal VJ. Reversible differentiation of myofibroblasts by MyoD. Exp Cell Res 2011;317:1914–21. doi:10.1016/j.yexcr.2011.03.016.

[31] Sapitro J, Dunmire JJ, Scott SE, Sutariya V, Geldenhuys WJ, Hewit M, et al. Suppression of transforming growth factor-β effects in rabbit subconjunctival fibroblasts by activin receptor-like kinase 5 inhibitor. Mol Vis 2010;16:1880–92.

[32] Gonzalez-Cadavid NF, Rajfer J. Treatment of Peyronie's disease with PDE5 inhibitors: An antifibrotic strategy. Nat Rev Urol 2010;7:215–21. doi:10.1038/nrurol.2010.24.

[33] Ralph DJ, Brooks MD, Bottazoo GF, Pryor JP. The Treatment of Peyronie's Disease with

Tamoxifen. Br J Urol 1992:648–51.

[34] Palmieri A, Imbimbo C, Creta M, Verze P, Fusco F, Mirone V. Tadalafil once daily and extracorporeal shock wave therapy in the management of patients with Peyronie's disease and erectile dysfunction: Results from a prospective randomized trial. Int J Androl 2012;35:190–5. doi:10.1111/j.1365-2605.2011.01226.x.

[35] Ozturk U, Yesil S, Goktug HNG, Gucuk A, Tuygun C, Sener NC, et al. Effects of sildenafil treatment on patients with Peyronie's disease and erectile dysfunction. Irish J Med Sci (1971 -) 2014;183:449–53. doi:10.1007/s11845-013-1036-5.

[36] Dell'Atti L. Tadalafil once daily and intralesional verapamil injection: A new therapeutic direction in Peyronie's disease. Urol Ann 2015;7:345–9. doi:10.4103/0974-7796.152048.

[37] Park TY, Jeong HG, Park JJ, Chae JY, Kim JW, Oh MM, et al. The Efficacy of Medical Treatment of Peyronie's Disease: Potassium Para-Aminobenzoate Monotherapy vs. Combination Therapy with Tamoxifen, L-Carnitine, and Phosphodiesterase Type 5 Inhibitor. World J Mens Health 2016;34:40–6. doi:10.5534/wjmh.2016.34.1.40.

[38] Zenzmaier C, Kern J, Sampson N, Heitz M, Plas E, Untergasser G, et al. Phosphodiesterase type 5 inhibition reverts prostate fibroblast-to- myofibroblast Trans-differentiation. Endocrinology 2012;153:5546–55. doi:10.1210/en.2012-1431.

[39] Jiang HS, Zhu LL, Zhang Z, Chen H, Chen Y, Dai YT. Estradiol attenuates the TGF-β1-induced conversion of primary TAFs into myofibroblasts and inhibits collagen production and myofibroblast contraction by modulating the Smad and Rho/ROCK signaling pathways. Int J Mol Med 2015;36:801–7. doi:10.3892/ijmm.2015.2288.

[40] Luo F, Ishigami M, Achiwa K, Ishizu Y, Kuzuya T, Honda T, et al. Raloxifene Ameliorates Liver Fibrosis of Nonalcoholic Steatohepatitis Induced by Choline-Deficient High-Fat Diet in Ovariectomized Mice. Dig Dis Sci 2015. doi:10.1007/s10620-015-3660-6.

[41] Dellê H, Rocha JRC, Cavaglieri RC, Vieira JM, Malheiros DMAC, Noronha IL. Antifibrotic effect of tamoxifen in a model of progressive renal disease. J Am Soc Nephrol 2012;23:37–48. doi:10.1681/ASN.2011010046.

[42] Hardman MJ, Emmerson E, Campbell L, Ashcroft GS. Selective estrogen receptor modulators accelerate cutaneous wound healing in ovariectomized female mice. Endocrinology 2008;149:551–7. doi:10.1210/en.2007-1042.

[43] Ryu SH, Chung YH, Lee JK, Kim JA, Shin JW, Jang MK, et al. Antifibrogenic effects of tamoxifen

in a rat model of periportal hepatic fibrosis. Liver Int 2009;29:308–14. doi:10.1111/j.1478-3231.2008.01811.x.

[44] Kim D, Lee AS, Jung YJ, Yang KH, Lee S, Park SK, et al. Tamoxifen ameliorates renal tubulointerstitial fibrosis by modulation of estrogen receptor α-mediated transforming growth factor-β1/Smad signaling pathway. Nephrol Dial Transplant 2014;29:2043–53. doi:10.1093/ndt/gfu240.

[45] Carthy JM, Sundqvist A, Heldin A, van Dam H, Kletsas D, Heldin CH, et al. Tamoxifen Inhibits TGF-β-Mediated Activation of Myofibroblasts by Blocking Non-Smad Signaling Through ERK1/2. J Cell Physiol 2015;230:3084–92. doi:10.1002/jcp.25049.

[46] Hu D, Hughes MA, Cherry GW. Topical tamoxifen - A potential therapeutic regime in treating excessive dermal scarring? Br J Plast Surg 1998;51:462–9. doi:10.1054/bjps.1997.0100.

[47] Gragnani A, Warde M, Furtado F, Ferreira LM. Topical tamoxifen therapy in hypertrophic scars or keloids in burns. Arch Dermatol Res 2010;302:1–4. doi:10.1007/s00403-009-0983-1.

[48] Pierpont MG, Bhalla YN, Desai R, Robson KC, Payne MC. Downregulation of Scar Fibroblasts by Antineoplastic Drugs: A Potential Treatment for Fibroproliferative Disorders. Surg Sci 2016;7:258–71. doi:10.4236/ss.2016.76037.

[49] Kuhn MA, Wang X, Payne WG, Ko F, Robson MC. Tamoxifen Decreases Fibroblast Function and Downregulates TGFβ2 in Dupuytren's Affected Palmar Fascia. J Surg Res 2002;103:146–52. doi:10.1006/JSRE.2001.6350.

[50] Sapino A, Pietribiasi F, Bussolati G, Marchisio PC. Estrogen- and Tamoxifen-induced Rearrangement of Cytoskeletal and Adhesion Structures in Breast Cancer MCF-7 Cells Estrogen- and Tamoxifen-induced Rearrangement of Cytoskeletal and Adhesion Structures in Breast Cancer MCF-7 Cells. Cancer Res 1986;46:2526–31.

[51] Acconcia F, Barnes CJ, Kumar R. Estrogen and tamoxifen induce cytoskeletal remodeling and migration in endometrial cancer cells. Endocrinology 2006;147:1203–12. doi:10.1210/en.2005-1293.

[52] Cortes E, Lachowski D, Rice A, Thorpe SD, Robinson B, Yeldag G, et al. Tamoxifen mechanically deactivates hepatic stellate cells via the G protein-coupled estrogen receptor. Oncogene 2019;38:2910–22. doi:10.1038/s41388-018-0631-3.

[53] Valente EGA, Vernet D, Ferrini MG, Qian A, Rajfer J, Gonzalez-Cadavid NF. L-Arginine and phosphodiesterase (PDE) inhibitors counteract fibrosis in the Peyronie's fibrotic plaque and

related fibroblast cultures. Nitric Oxide - Biol Chem 2003;9:229–44. doi:10.1016/j.niox.2003.12.002.

[54] Kraft PJ, Haynes-Johnson D, Bhattacharjee S, Lundeen SG, Qiu Y. Altered activities of cyclic nucleotide phosphodiesterases and soluble guanylyl cyclase in cultured RFL-6 cells. Int J Biochem Cell Biol 2004;36:2086–95. doi:10.1016/J.BIOCEL.2004.04.006.

[55] Dunkern TR, Feurstein D, Rossi GA, Sabatini F, Hatzelmann A. Inhibition of TGF-β induced lung fibroblast to myofibroblast conversion by phosphodiesterase inhibiting drugs and activators of soluble guanylyl cyclase. Eur J Pharmacol 2007;572:12–22. doi:10.1016/j.ejphar.2007.06.036.

[56] Ford CHJ, Al-Bader M, Al-Ayadhi B, Francis I. Reassessment of estrogen receptor expression in human breast cancer cell lines. Anticancer Res 2011;31:521–7.

[57] Palmieri C, Saji S, Sakaguchi H, Cheng G, Sunters A, O'Hare M, et al. The expression of oestrogen receptor (ER)-beta and its variants, but not ER alpha, in adult human mammary fibroblasts. J Mol Endocrinol 2004;33:35–50.

[58] Hopp TA, Weiss HL, Parra IS, Cui Y, Osborne CK, Fuqua SAW. Low levels of estrogen receptor beta protein predict resistance to tamoxifen therapy in breast cancer. Clin Cancer Res 2004;10:7490–9. doi:10.1158/1078-0432.CCR-04-1114.

[59] Gruvberger-Saal SK, Bendahl P-O, Saal LH, Laakso M, Hegardt C, Edén P, et al. Estrogen receptor beta expression is associated with tamoxifen response in ERalpha-negative breast carcinoma. Clin Cancer Res 2007;13:1987–94. doi:10.1158/1078-0432.CCR-06-1823.

[60] Kadioglu A, Tefekli A, Erol B, Oktar T, Tunc M, Tellaloglu S. A Retrospective Review of 307 Men With Peyronie's Disease. J Urol 2002;168:1075–9. doi:10.1016/S0022-5347(05)64578-8.

[61] Mulhall JP, Schiff J, Guhring P. An Analysis of the Natural History of Peyronie's Disease. J Urol 2006;175:2115–8. doi:10.1016/S0022-5347(06)00270-9.

[62] Berookhim BM, Choi J, Alex B, Mulhall JP. Deformity stabilization and improvement in men with untreated Peyronie's disease. BJU Int 2014;113:133–6. doi:10.1111/bju.12346.

[63] Lakota K, Wei J, Carns M, Hinchcliff M, Lee J, Whitfield ML, et al. Levels of adiponectin, a marker for PPAR-gamma activity, correlate with skin fibrosis in systemic sclerosis: Potential utility as biomarker? Arthritis Res Ther 2012;14. doi:10.1186/ar3827.

[64] Biagiotti G, Cavallini G. Acetyl-L-carnitine vs tamoxifen in the oral therapy of Peyronie's

disease: A preliminary report. BJU Int 2001;88:63–7. doi:10.1046/j.1464-410X.2001.02241.x.

[65] Jiang F, Zhang Z, Zhang Y, Wu J, Yu L, Liu S. L-carnitine ameliorates the liver inflammatory response by regulating carnitine palmitoyltransferase I-dependent PPARγ signaling. Mol Med Rep 2016;13:1320–8. doi:10.3892/mmr.2015.4639.

[66] Lakatos HF, Thatcher TH, Kottmann RM, Garcia TM, Phipps RP, Sime PJ. The role of PPARs in lung fibrosis. PPAR Res 2007. doi:10.1155/2007/71323.

[67] Du W, Liang H, Gao X, Li X, Zhang Y, Pan Z, et al. MicroRNA-328, a Potential Anti-Fibrotic Target in Cardiac Interstitial Fibrosis. Cell Physiol Biochem 2016;39:827–36. doi:10.1159/000447793.

[68] Biernacka A, Dobaczewski M, Frangogiannis NG. TGF-β signaling in fibrosis. Growth Factors 2011;29:196–202. doi:10.3109/08977194.2011.595714.

[69] Murphy-Ullrich JE, Suto MJ. Thrombospondin-1 regulation of latent TGF-β activation: A therapeutic target for fibrotic disease. Matrix Biol 2018;68–69:28–43. doi:10.1016/J.MATBIO.2017.12.009.

[70] Sweetwyne MT, Murphy-Ullrich JE. Thrombospondin1 in tissue repair and fibrosis: TGF-β-dependent and independent mechanisms. Matrix Biol 2012;31:178–86. doi:10.1016/j.matbio.2012.01.006.

[71] Phelan MW, Forman LW, Perrine SP, Faller D V. Hypoxia increases thrombospondin-1 transcript and protein in cultured endothelial cells. J Lab Clin Med 1998;132:519–29. doi:10.1016/S0022-2143(98)90131-7.

[72] Hugo C, Shankland SJ, Pichler RH, Couser WG, Johnson RJ. Thrombospondin 1 precedes and predicts the development of tubulointerstitial fibrosis in glomerular disease in the rat. Kidney Int 1998;53:302–11. doi:10.1046/j.1523-1755.1998.00774.x.

[73] Cabrini MR, Sezen SF, Lagoda G, Segal RL, Feng Z, Andreoni C, et al. Fibrotic protein expression profiles in penile tissue of patients with erectile dysfunction. Urology 2013;82:975.e1-975.e6. doi:10.1016/j.urology.2013.06.042.

Figure Legends:

Figure 1: PDE5i and SERM cannot reverse ASMA expression after 72h of TGF-β1 pre-treatment of TA-derived cells. A) Effect of vardenafil on ASMA expression. TA-derived cells were pre-treated with 10 ng/mL of TGF-β1 for 72h and then exposed to various concentrations (0.1-1,000 μM) of vardenafil. B) Effect of tamoxifen on ASMA expression. TA-derived cells were pre-treated with TGF-β1 for 72h and then exposed to various concentrations (0.018-54 μM) of tamoxifen. ASMA staining was normalised to DNA staining (cell viability). Data points were plotted as average ± SEM of ASMA/DNA staining ratio obtained from Odyssey infra-red imager. N=3

Figure 2: PDE5i and SERMs do not reduce ECM production after 72h of TGF-β1 pre-treatment of TA-derived cells. TA-derived cells were pre-treated with 10ng/mL of TGF-β1 for 72h and then exposed to various concentrations of vardenafil (0.03-100 μM; blue), tamoxifen (0.018-54 μM; red), or SB-505124 (0.03-100 μM; grey). 8 days after treatment cells were lysed and ECM content was quantified. ECM proteins included Col I (A), Col V (B), Col III (C), and fibronectin (D). Protein was normalised to DNA staining before lysis. Data points were plotted as average ± SEM of protein/DNA staining ratio obtained from Odyssey infra-red imager. N=3

Figure 3: SERM but not PDE5i can reduce collagen contraction after 72h of TGF-β1 pre-treatment of TA-derived cells. TA-derived cells were pre-treated with 10 ng/mLTGF-β1 for 72h and then exposed to various concentrations of A) SB-505124 (1, 3, 10 μM), B) vardenafil (10, 30, 100 μM), C) tamoxifen (1, 3, 10 μM). 3 days after treatment collagen lattices were released from the wall of the well and contraction was observed over an 8h period. Data presented as percentage of maximum collagen contraction compared to vehicle control (DMSO), data points plotted as mean ± SEM. Statistical analysis using student's t-test with *p<0.05 vs vehicle control. N=3

Figure 4: Quantification of PDE5A, ER-α and ER-β after 72h of TGF-β1 treatment of TA-derived cells. TA-derived cells were left untreated or treated with 10 ng/mL of TGF-β1 for 72h. A) Quantification of PDE5A using ICE. Data points plotted as mean ± SEM. Blocking peptide and positive control cell line MCF7 used for accuracy. Statistical analysis using student's t-test with *p<0.05 vs untreated. N=3. B) Quantification of ER-α using ICE. Data points plotted as mean ± SEM. Blocking peptide and positive control cell line MCF7 used for accuracy. Statistical analysis using student's t-test with *p<0.05 vs

untreated. N=3. C) Quantification of ER-β using ICE. Data points plotted as mean ± SEM. Blocking peptide and positive control cell line MCF7 used for accuracy. Statistical analysis using student's t-test with *p<0.05 vs untreated. N=3

Figure 5: Effect of PDE5i at various time points after TGF-β1 treatment. TA-derived cells were treated with TGF-β1 for 24h (A), 36h (B) or 48h (C). After indicated incubation period, TGF-β1 was removed and cells were treated with various concentration (0.1-1,000 µM) of vardenafil. ASMA staining was assessed 72h after initial TGF-β1 treatment. ASMA staining was normalised to DNA staining (cell viability). Data points were plotted as average ± SEM of ASMA/DNA staining ratio obtained from Odyssey infra-red imager. N=3

Figure 6: Effect of SERM at various time points after TGF-β1 treatment. TA-derived cells were treated with TGF-β1 for 24h (A), 36h (B) or 48h (C). After indicated incubation period, TGF-β1 was removed and cells were treated with various concentration (0.018-54 µM) of tamoxifen. ASMA staining was assessed 72h after initial TGF-β1 treatment. ASMA staining was normalised to DNA staining (cell viability). Data points were plotted as average ± SEM of ASMA/DNA staining ratio obtained from Odyssey infra-red imager. N=3

Figure 7: Effect of TGF-β1 exposure time on mRNA and protein expression of ASMA, PDE5A and ERs. TA-derived cells were treated with TGF-β1 for 24h, 36h, 48h or 72h. Expression of mRNA was assessed for ACTA (A), PDE5A (B), ER1 (C), and ER2 (D). Expression patterns of genes at 24h, 36h, 48h and 72h. Results are plotted as expression fold difference compared to t=0 in response to TGF-ß relative to the expression of the reference gene GAPDH. Pink horizonal lines mark the 3-fold up- or down-regulation levels, as previously suggested as limits of significance. Each time point represents the mean fold difference ± range. Protein expression of ASMA (E), PDE5A (F) and ER-β (G) was quantified. ICE was used to determine Protein/DNA staining ratio. Data points were plotted as average ± SEM of ASMA/DNA staining ratio obtained from Odyssey infra-red imager. Statistical analysis performed using one-way ANOVA with multiple comparisons. *p<0.05 vs control column. #p<0.05 vs 24h column. N=3.

Figure 8: Effect of TGF-β1 exposure on various target genes. Expression patterns of PPARγ (A), TGFß-R3 (B) and ThsB (C) at 24h, 36h, 48h and 72h. Results are plotted as expression fold difference

compared to t=0 in response to TGF-ß relative to the expression of the reference gene GAPDH. Pink horizonal lines mark the 3-fold up- or down-regulation levels, as previously suggested as limits of significance. Each time point represents the mean fold difference ± range.

Supplementary Figure 1: Immunocytochemistry to confirm In-Cell ELISA protein quantification. TA-derived cells were left untreated or exposed to 10 ng/mL of TGF-β1 for 72h. Protein of interest stained in green, nuclear staining in red. Representative images of PDE5A stainings captured at 200x magnification for untreated cells (A) and TGF-β1 treated cells (B). (C) Quantification of PDE5A stainings. Three independent images were quantified. Statistical analysis using Students t-test with *p<0.05. Representative images of ER-α stainings captured at 200x magnification for untreated TA-derived cells (D), TGF-β1 treated TA-derived cells (E) and positive control cell line MCF7 (F). Representative images of ER-β stainings captured at 200x magnification for untreated cells (G) and TGF-β1 treated cells (H). (I) Quantification of ER-β stainings. Three independent images were quantified. Statistical analysis using Students t-test with *p<0.05. (J, K) Positive control cell line MCF7 stained for PDE5A (J) and ER-β (K).

Supplementary Figure 2: Effect of TGF-β1 removal in 72h incubation period. Cells were treated with TGF-β1 the day after seeding. TGF-β1 was removed after 24h, 36h, 48h, or 72h and ASMA protein expression was quantified 72h after the initial exposure. ASMA expression was normalised to DNA staining and data points plotted as mean ± SEM of ASMA/DNA staining ratio obtained from Odyssey infra-red imager. N=3

Supplementary Figure 3: Effect of SB-505124 at various time points after TGF-β1 treatment. TA-derived cells were treated with TGF-β1 for 24h (A), 36h (B), 48h (C), or 72h. After indicated incubation period, TGF-β1 was removed and cells were treated with various concentration (0.03-100 µM) of SB-505124. ASMA staining was assessed 72h after initial TGF-β1 treatment. ASMA staining was normalised to DNA staining (cell viability). Data points were plotted as average ± SEM of ASMA/DNA staining ratio obtained from Odyssey infra-red imager. N=3

Supplementary Figure 4: Verification of GAPDH as valid housekeeping gene. Column bar graph of GAPDH expression at various time points after TGF-ß treatment relative to the no treatment control.

Duplicate PCR assays were performed on RT reactions carried out in duplicate on RNA extracted from one individual and a third RT reaction carried out on RNA extracted from a second individual. Each bar represents the mean Cq difference ± SD.

Supplementary Figure 5: Additional marker genes investigated in TGF-β1 time course experiments. Expression patterns of GPER4 (A), BIRC5 (B) and GPER2 (C), IGF1 (D) and IGFBP3 (E) at 24h, 36h, 48h and 72h. Results are plotted as expression fold difference compared to t=0 in response to TGF-ß relative to the expression of the reference gene GAPDH. Pink horizonal lines mark the 3-fold up- or down-regulation levels, as previously suggested as limits of significance. Each time point represents the mean fold difference ± range.

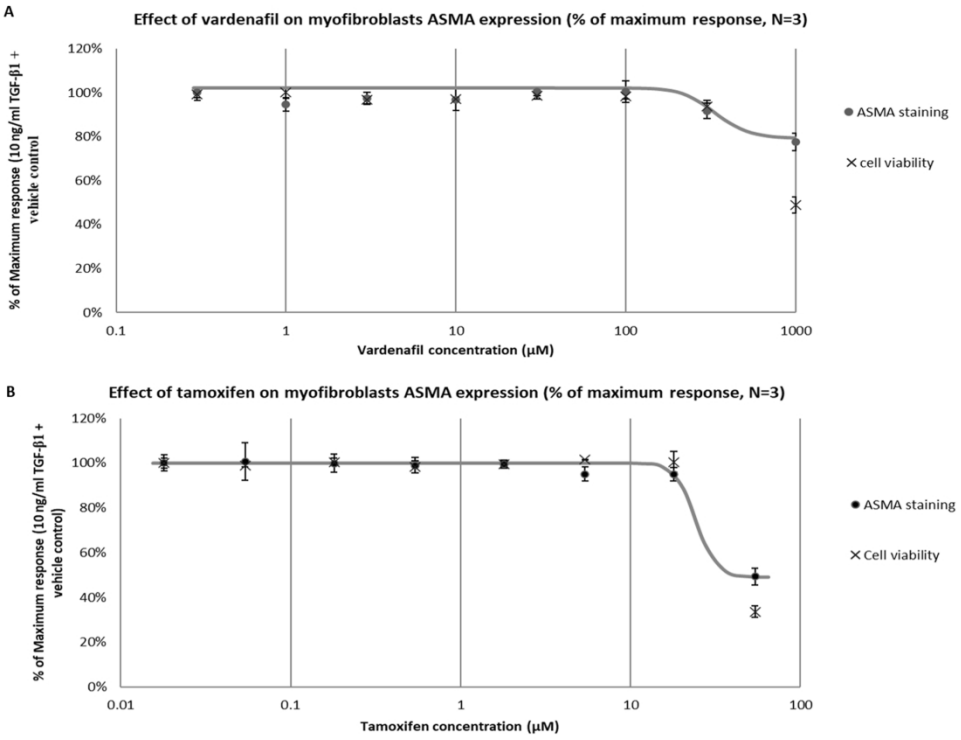

Figure 1

250x190mm (300 x 300 DPI)

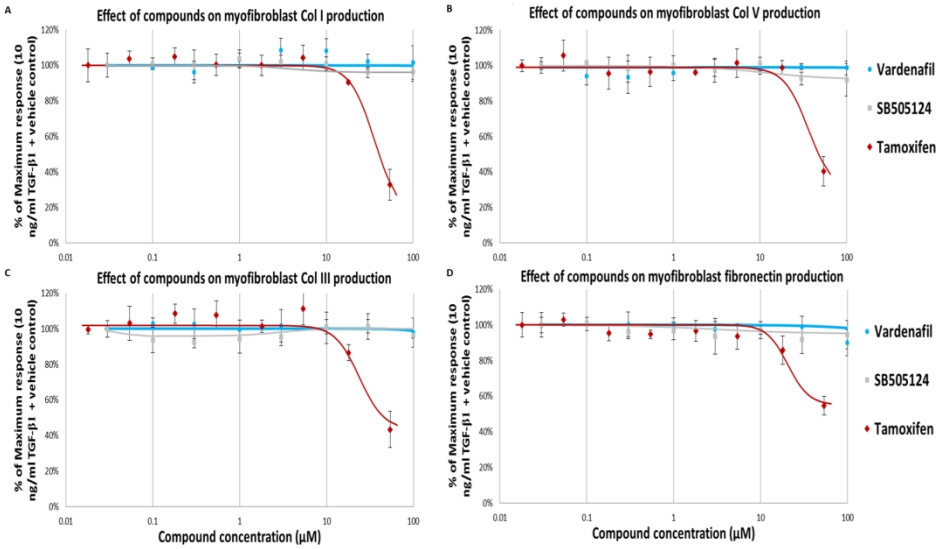

Figure 2

339x190mm (300 x 300 DPI)

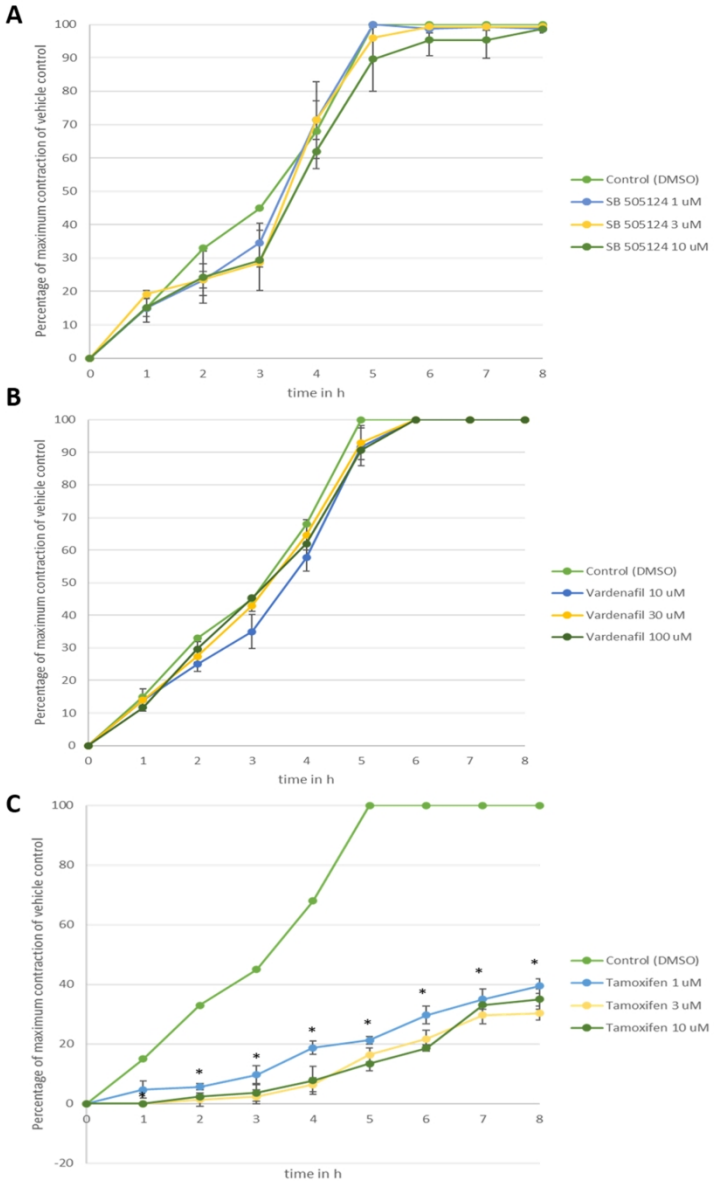

Figure 3

185x274mm (300 x 300 DPI)

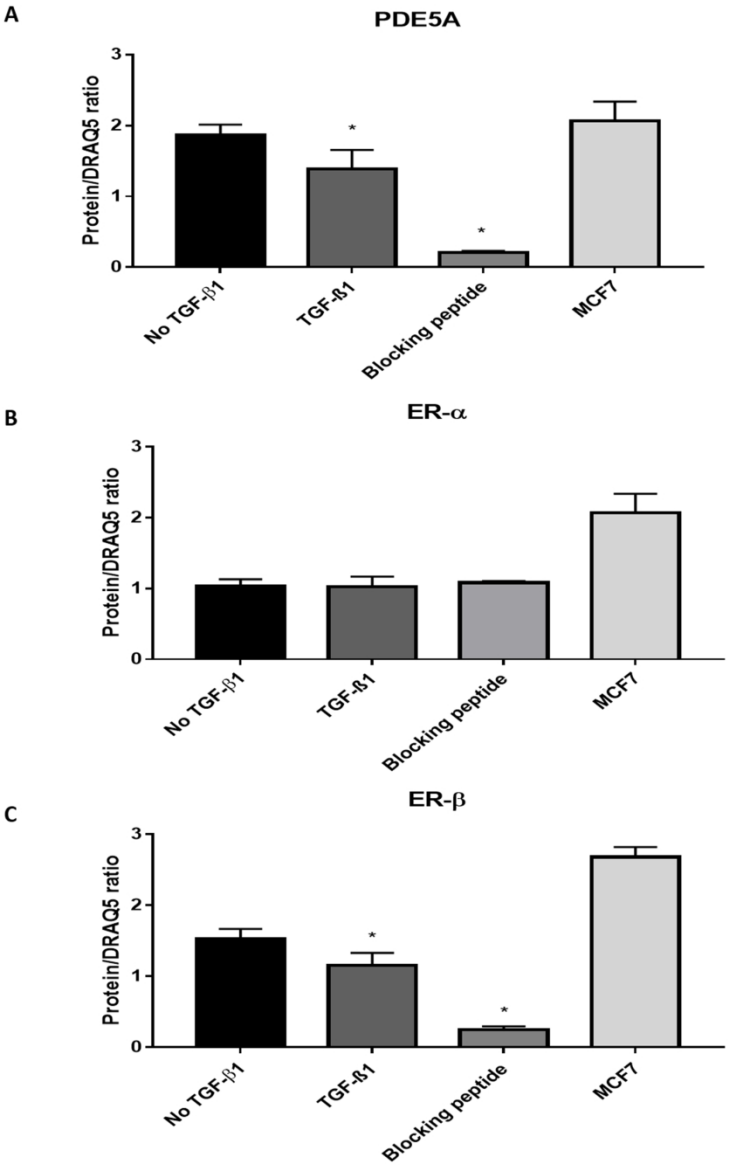

Figure 4

190x274mm (300 x 300 DPI)

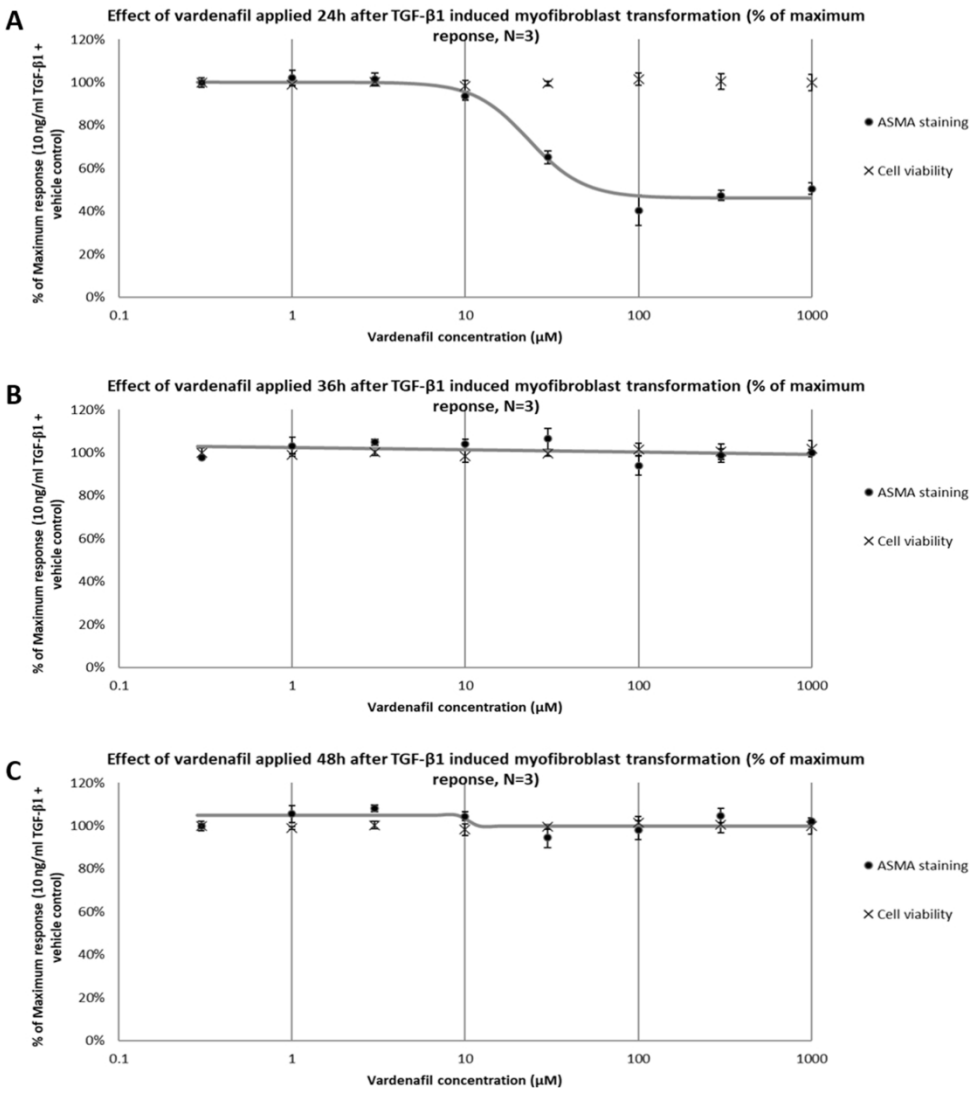

Figure 5

186x215mm (300 x 300 DPI)

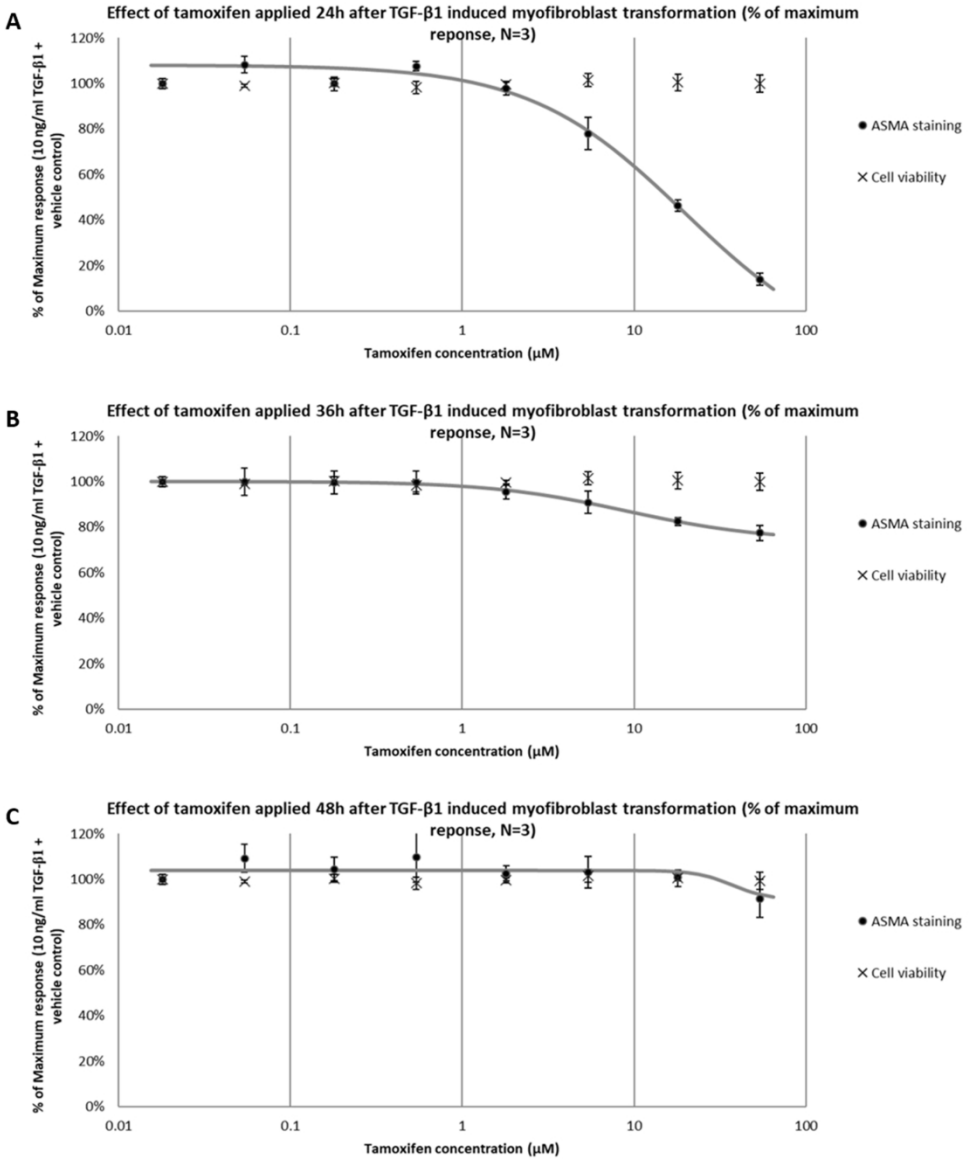

Figure 6

188x223mm (300 x 300 DPI)

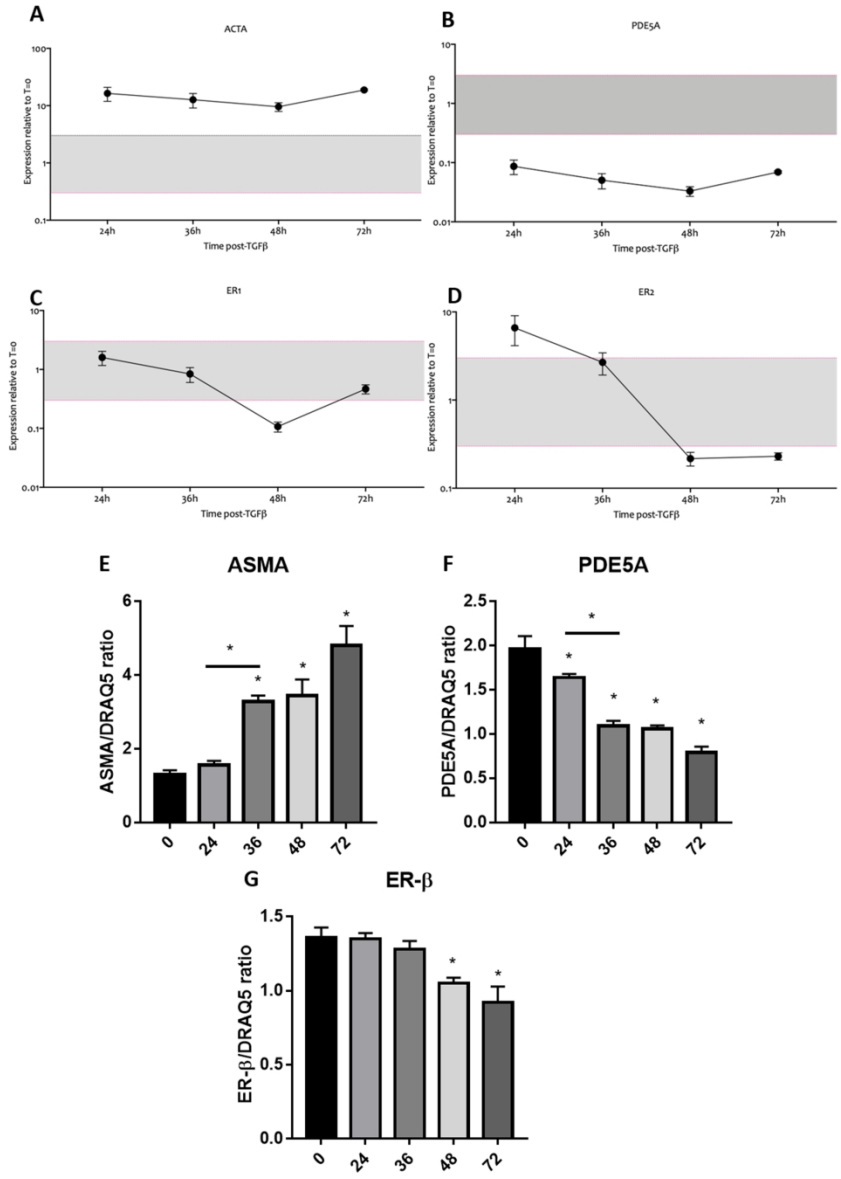

Figure 7

192x275mm (300 x 300 DPI)

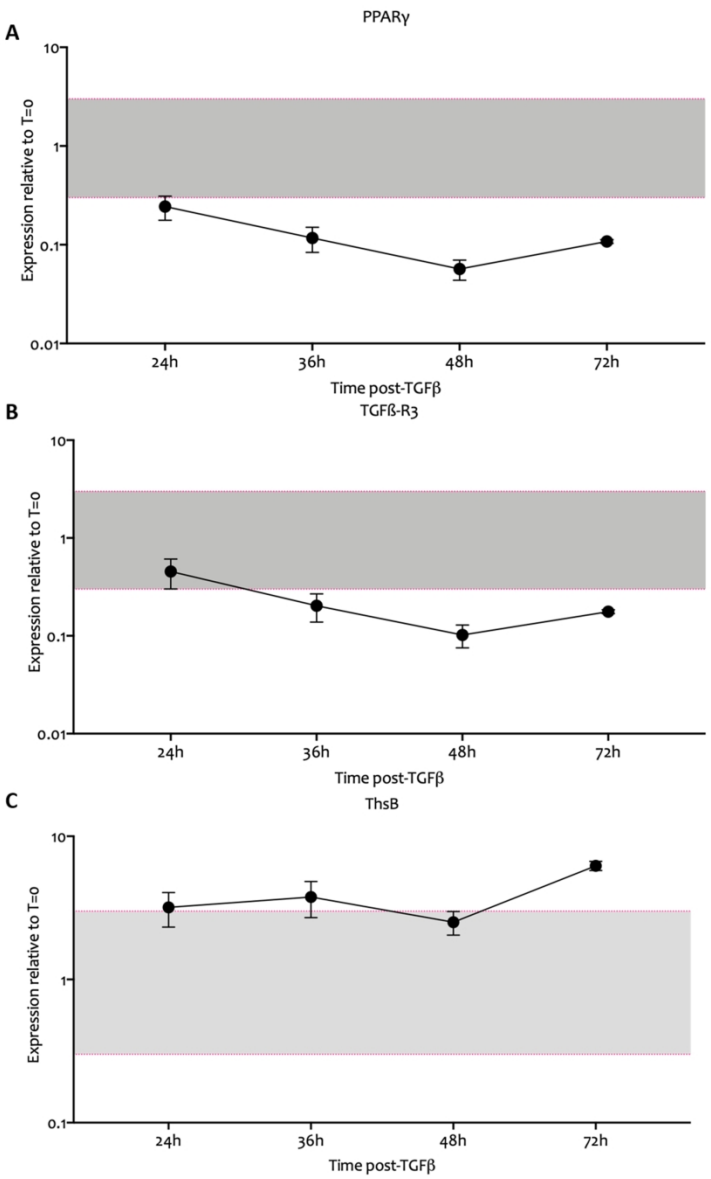

Figure 8

190x282mm (300 x 300 DPI)

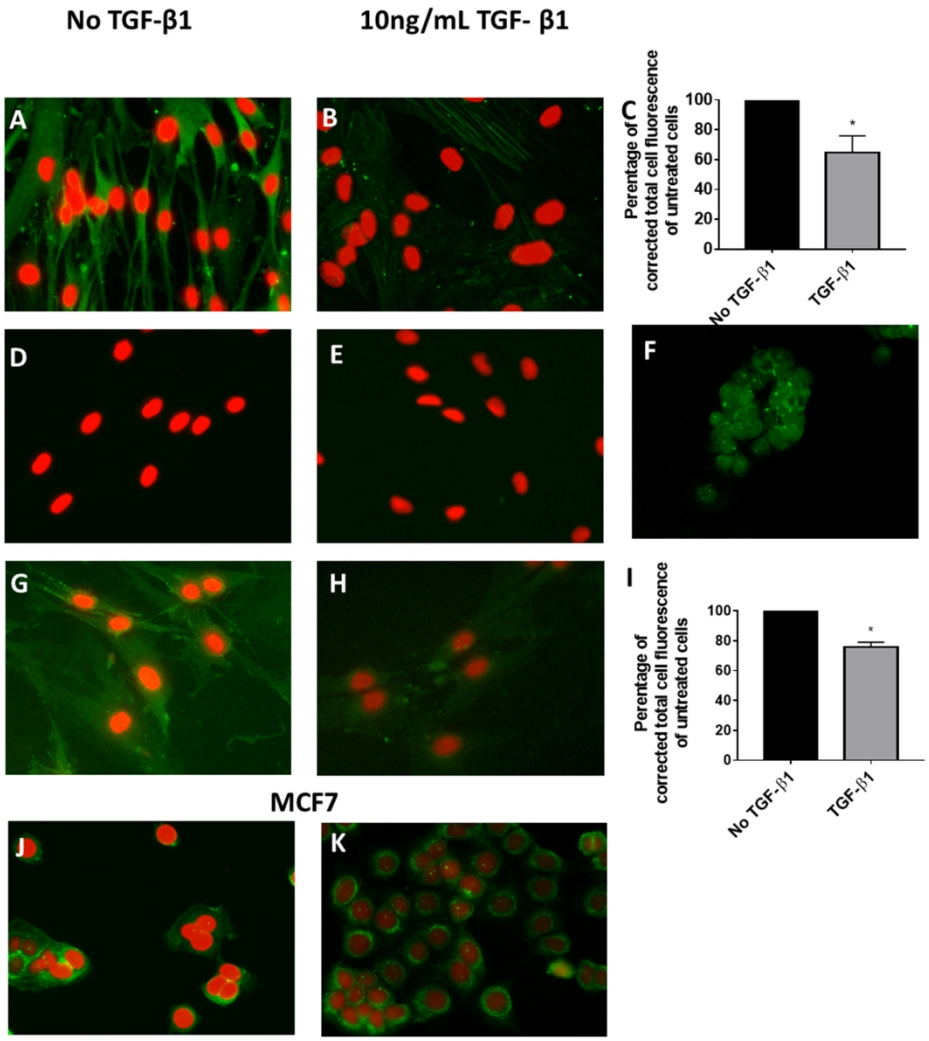

Supplementary Figure 1

190x205mm (300 x 300 DPI)

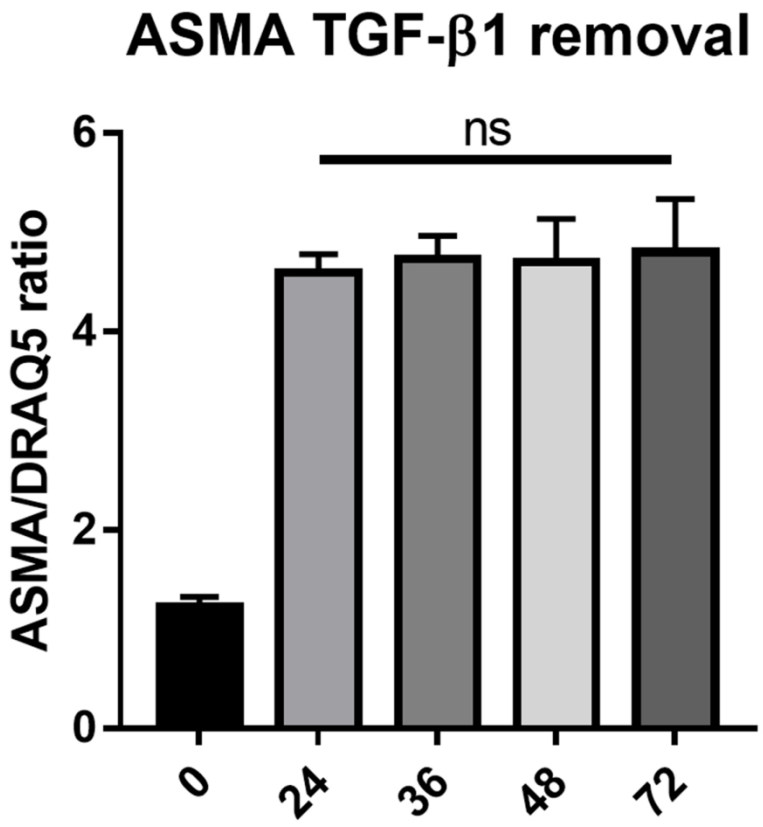

Supplementary Figure 2

161x164mm (300 x 300 DPI)

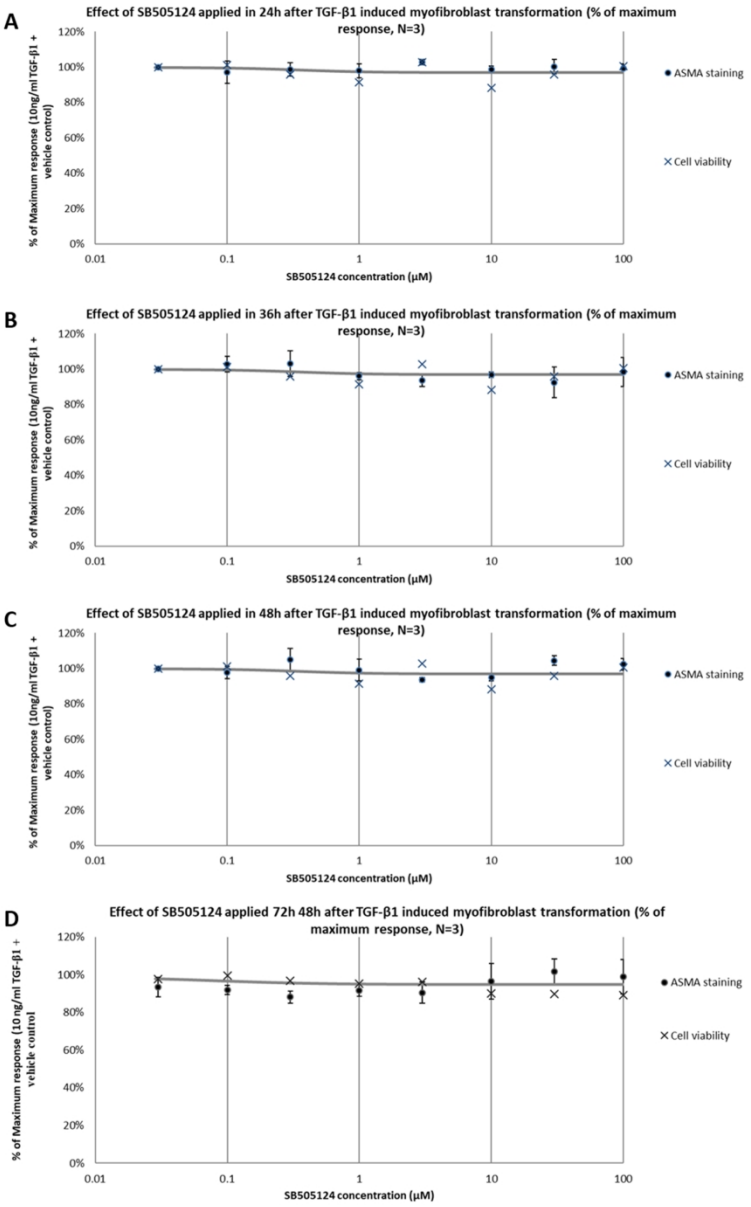

Supplementary Figure 3

187x274mm (300 x 300 DPI)

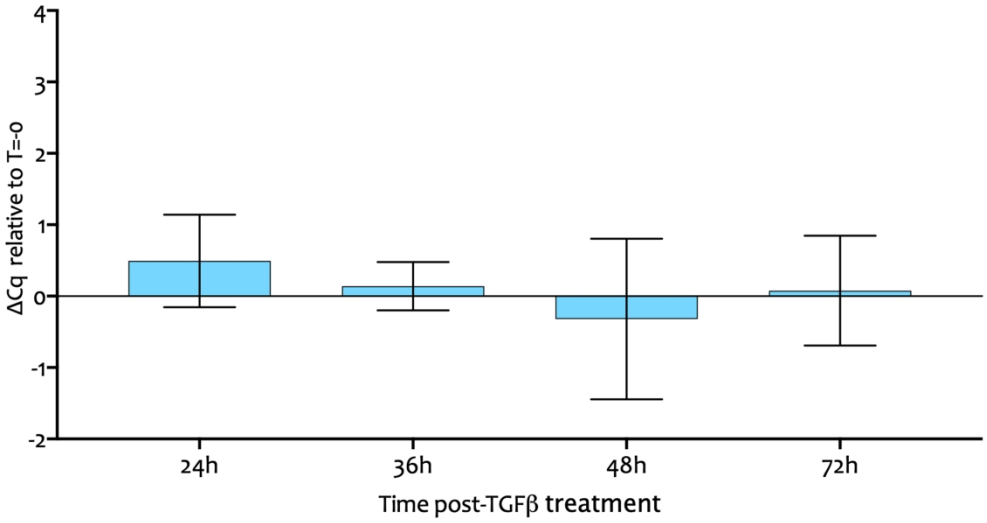

Supplementary Figure 4

380x208mm (300 x 300 DPI)

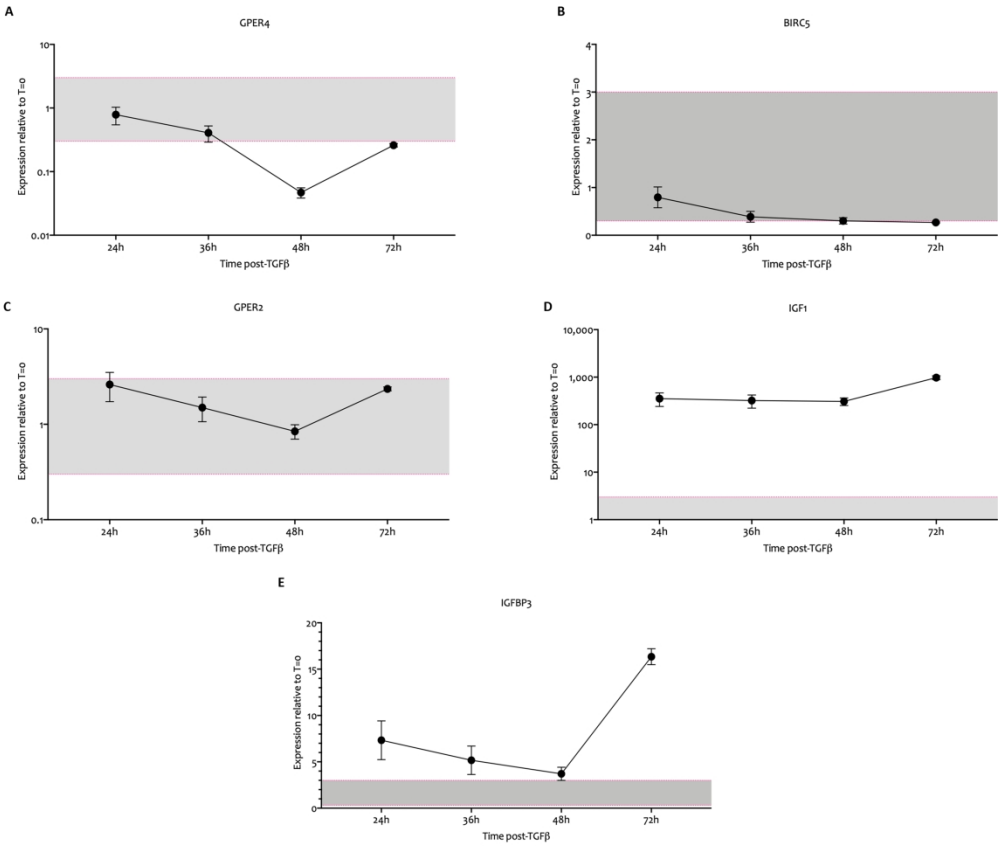

Supplementary Figure 5

389x339mm (300 x 300 DPI)